PCCP

View Online / Journal Homepage / Table of Contents for this issue
Dynamic Article Links

Cite this: *Phys. Chem. Chem. Phys.*, 2011, **13**, 15708–15713

www.rsc.org/pccp

PAPER

Molecular simulation of the binary mixture of 1–1–1–2–tetrafluoroethane and carbon dioxide†

Hainam Do, Richard J. Wheatley and Jonathan D. Hirst*

Received 4th May 2011, Accepted 8th July 2011
DOI: 10.1039/c1cp21419e

The refrigerant 1–1–1–2–tetrafluoroethane (R134a) is being phased out in Europe from 2011. This requires the adoption of alternatives, and the mixture of R134a with carbon dioxide (CO_2) is a promising candidate. However, limited experimental data currently stymie evaluation of its performance in industrial applications. In this paper, we employ atomistic force fields and the configurational-bias Monte Carlo technique to study the vapour–liquid equilibrium of this mixture. We also characterize the microscopic structure of the mixture, which is not readily available from experiments. At 272 K and 11.55 bar, the average coordination number of the first solvation shell of R134a is 11 and that of CO_2 is eight. CO_2 does not alter the structure of R134a, but its structure is slightly changed, due to the presence of R134a. All pair interactions are sensitive to pressure and are more structured at lower pressure. CO_2 prefers to form clusters of two in the mixture and highly extended or percolating clusters are not found.

I. Introduction

Replacement of conventional chlorofluorohydrocarbon refrigerants is an urgent issue to be addressed within the schedule of the amended Montreal Protocol.[1] Moreover, from January 2011, the European Union has banned the use of refrigerants that have global warming potentials higher than 150 in automotive heating ventilation and air conditioning systems. This means that the commonly used tetrafluoroethane (R134a) will be phased out. Thus, there is the need to adopt new refrigerants or mixtures of refrigerants that comply with the European Union legislation. Carbon dioxide (CO_2) has a very low global warming potential, and has received much attention as a fluid that can be used in combination with other refrigerants to reduce flammability and toxicity hazards. It could be mixed with R134a to form a new refrigerant that meets the requirements of the European Union legislation. Vapour–liquid equilibrium (VLE) data are essential for the identification of mixtures with suitable thermodynamic properties. Unfortunately, only little information on the thermophysical properties of this mixture is available. Thus, even empirical equations of state, such as the Peng–Robinson equation of state,[2] cannot be used with confidence, as there are not enough data to evaluate their parameters with sufficient statistical significance.

In recent years, molecular simulation based on molecular modelling has emerged as an important complement to experiment for obtaining reliable thermodynamic and transport properties. In addition, it can provide an insight into the microscopic structure of the systems, which cannot be measured experimentally. Under conditions in which experiment cannot access, computer simulations can be readily conducted.[3] It is generally agreed that phase transitions are best treated by Monte Carlo simulation. Methods for predicting phase equilibria properties from a detailed atomistic simulation have evolved rapidly in recent years. Such ;approaches fall into two broad categories: simulations without interfaces and biased sampling techniques. Foremost in the former category are methods such as Gibbs ensemble Monte Carlo (GEMC)[4–6] and Gibbs–Duhem integration.[7] Other techniques, such as the expanded ensemble method[8] and histogram reweighting grand canonical Monte Carlo[9] fall into the second category and are less straightforward to implement than those in the first category. Recently, several new approaches based on a uniform sampling of the extensive variables have been reported.[10–19] These include the Wang–Landau sampling,[10,11] which explores configurational space such that each energy is visited with an equal probability, including the two coexisting phases and the interface. Therefore, they are ideal for the study of phase transitions, unlike standard Boltzmann sampling, which only favours the low energy region of the configurational space. However, these methods are not straightforward for the study of multi-component systems.

The configurational-bias sampling technique[20–22] has significantly broadened the range of systems for which phase behaviour can be studied. This has addressed many technological issues, for example in determination of VLE of multi-components at high pressure, and the critical parameters of heavy hydrocarbons, which is very important in the petro-chemical industry.[23–29] Simulations of VLE are sensitive to the details of

School of Chemistry, University of Nottingham, University Park, Nottingham, NG7 2RD, UK
† Electronic supplementary information (ESI) available. See DOI: 10.1039/c1cp21419e

the force fields. Therefore, research to make transferable force fields to predict VLE properties of important industrial substances has been an active field.[30–35] For pure systems, force field parameters are optimized to reproduce experimental data, and for mixtures force field parameters are constructed using a combining rule. Such parameters can also be determined from *ab initio* calculations, but these are relatively rare, due to high computational cost.

A number of force fields for R134a have been proposed.[36–41] However, these either are highly simplified (consisting of a two-centre Lennard-Jones potential,[41] which provides only limited structural information), or use less standard functional forms to describe the non-bonded interactions,[36–38] which are not compatible with popular 12-6 Lennard-Jones CO_2 force fields, such as the EPM model.[42] Recently, Peguin *et al.*[43,44] proposed an all-atom force field for R134a using a Lennard-Jones 12-6 function to describe the repulsion and dispersion energy and point charges to describe the Coulombic energy. This force field accurately predicts the thermophysical properties of R134a, but there is no guarantee that it can predict the VLE properties of multi-component systems. The aim of our work is to investigate whether this new force field together with the well-known force field EPM for CO_2 can accurately predict the thermophysical properties of the industrially important mixture R134a + CO_2. The EPM model has been successfully used to predict thermophysical properties of various binary mixtures containing CO_2.[45,46]

The microscopic structure of the liquid mixture R134a + CO_2 is not yet fully accessible *via* experiment, but clearly underpins the mixture's behaviour at the macroscopic level. In this work, we take advantage of simulations. Studies along these lines have been performed for pure substances, including CO_2,[47–49] R134a,[50] methylene chloride,[51] and difluoromethane[52] and mixtures of small molecules, such as CO_2 + methane[46,53] and CO_2 + difluoromethane.[46] However, due to the lack of an accurate force field for R134a, such analysis has not yet been performed for R134a + CO_2. Therefore, we use simulations to probe the saturated liquid structure. We compare the structure of the liquid mixture with both pure R134a and pure CO_2 under the same conditions to investigate the influence of CO_2 on R134a and *vice versa*. The effect of pressure on the liquid structure is investigated and we characterise the size of CO_2 clusters in the mixture. The current study complements previous studies of mixtures that contain CO_2 and will provide insights of relevance to a broad range of mixtures of fluoroalkanes and CO_2.

II. Methods

The NPT version of the GEMC technique,[4,5] implemented in in-house software, is employed to calculate the VLE properties of the mixture. In addition, we employ the coupled–decoupled[54] configurational-bias MC (CBMC) technique to sample the conformation of R134a *via* a regrowth move and a CBMC particle swap move to enhance the probability of successful particle transfer. In our simulations, the established EPM potential for CO_2[42] is employed and combined with a recently published eight-centre Lennard-Jones plus charges model, which reproduces well the VLE of R134a.[43,44] For the Lennard-Jones interactions between unlike atoms, the Lorentz–Berthelot combining rules are used.

An equal number of molecules are placed at random positions in both boxes at the start of a simulation. The density and composition of each box are chosen initially to give a roughly equal partitioning of the particles between each box once equilibrium is reached. The binary mixture is simulated with 500 molecules in the system. Simulations consist of 100 000 MC cycles. The first 50 000 cycles are used to equilibrate the system. Each MC cycle comprises an average of one translation move and one rotation move per molecule, one volume move, 50 regrowth moves, 150 standard particle transfer moves, and 100 CBMC particle transfer moves. The growing procedure for R134a in the regrowth and the CBMC particle transfer moves are the same as our previous work (ESI†).[50] The production period of each simulation is divided into ten blocks, and the standard errors of the simulations are calculated from these blocks. A spherical cutoff, r_{cut}, of 12 Å between molecules is used to truncate the Lennard-Jones part of the potential energy and a tail correction[6] compensates for its long-range truncation. Ewald summation with tinfoil boundary conditions is used to calculate the electrostatic interactions.[55]

III. Results and discussion

A. Vapour–liquid equilibrium of R134a + CO_2

To allow comparison with the experimental data, NPT-GEMC simulations are carried out at 252 K, 272 K and 292 K. Overall, within the statistical uncertainties, the simulation results are in good agreement with experimental data.[1] The calculated and experimental P–x data are plotted in Fig. 1 (see also Tables S1–S3 in the ESI†). At 252 K, the simulations correctly predict the solubility of CO_2 in both phases over a

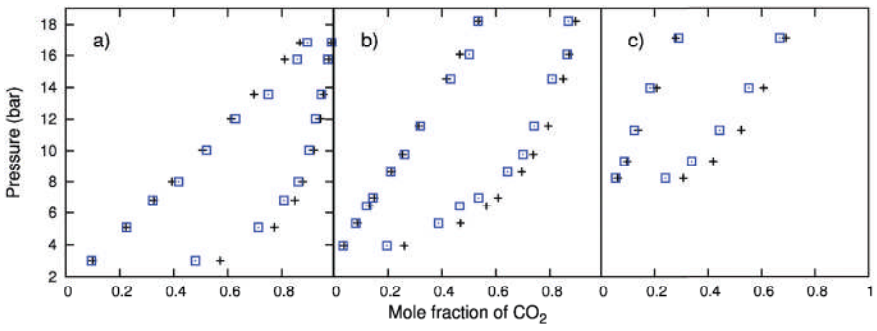

Fig. 1 Vapour–liquid equilibria of R134a + CO_2 at (a) 252 K, (b) 272 K, and (c) 292 K: simulation (squares) *versus* experimental data[1] (pluses). The error bars are very small and are not included.

wide range of saturated pressures. Fig. 1a shows that the simulations slightly overestimate the mole fraction of CO_2 in the liquid phase at high pressures and slightly underestimate it in the vapour phase at low pressures. The simulation results for 272 K are shown in Table S2 (ESI†) and Fig. 1b. The statistical uncertainties in the densities are similar to those of the system at 252 K. The simulations at 272 K underestimate the mole fraction of CO_2 in the vapour phase, but predict it correctly in the liquid phase at all simulated pressures. The deviations from experimental data for the vapour phase at this temperature are slightly larger than those at 252 K. The simulation results at 292 K are presented in Table S3 (ESI†) and the calculated and experimental P–x data are compared in Fig. 1c. The simulations correctly reproduce the experimental data for the solubility of CO_2 in the liquid phase at all simulated state points, but, as at 252 K and 272 K, they also underestimate the mole fraction of CO_2 in the vapour phase.

B. Microscopic structure

We consider the simulated data of the saturated liquid R134a + CO_2 mixture at 272 K and 11.55 bar as an example. Other states can be analysed analogously. Under these conditions, the ratio of CO_2 to R134a in the liquid phase is about 1 : 2. Questions arising here are: what is the structure of the liquid mixture under these conditions, *i.e.*, how are molecules packed together? What are their orientations? What is the influence of one component on the other? What is the preferred cluster size of CO_2 solute in R134a solvent? In this section, we address these questions.

We determined the distribution of the U_{ij} pair interaction energies of R134a–R134a, R134a–CO_2, and CO_2–CO_2 interactions in the saturated liquid mixture at 272 K and 11.55 bar (Fig. 2a). All of the curves in Fig. 2a have a shoulder on the left-hand side of the main peak. These shoulders are indicative of the association of the molecules in the liquid phase, which could arise from dipolar association[52] or simply induction and dispersion interactions. In order to have a clear picture of where these interactions occur, we analyse the probability distribution of these pair interactions as a function of the intermolecular distances (Fig. 2b–d). Fig. 2b–d show that the R134a–R134a, R134a–CO_2, and CO_2–CO_2 pair interactions occur at relatively short distances, within the first solvation shell of each type of interaction. The R134a–R134a pair interaction is the strongest and the CO_2–CO_2 pair interaction is the weakest.

The RDFs of the CO_2–CO_2, CO_2–R134a and R134a–R134a interactions at different pressures at 272 K are shown in Fig. 3. As the pressure increases, the height of the peak of the first

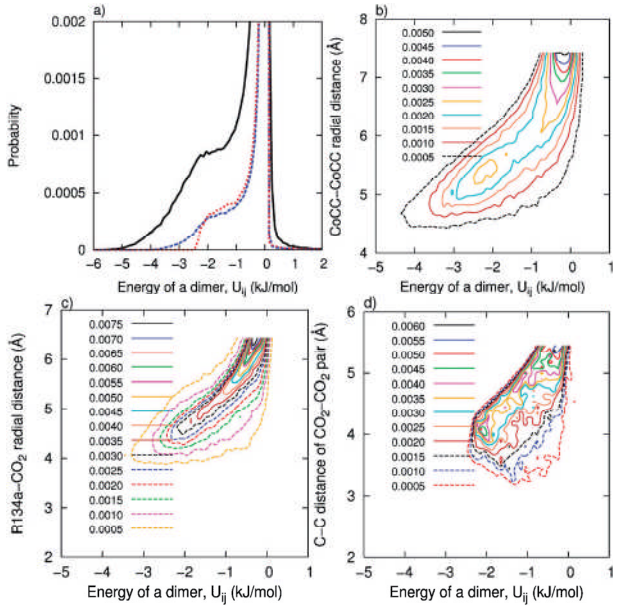

Fig. 2 (a) Probability distribution of the pair interaction energy of R134a–R134a (solid line), R134a–CO_2 (dashed line), and CO_2–CO_2 (dotted line). (b)–(d) are the distributions of the R134a–R234a, R134a–CO_2, CO_2–CO_2 pair interactions, respectively, at different distances at 272 K and 11.55 bar. We define the centre of the R134a molecule (CoCC) as the midpoint of the CC bond.

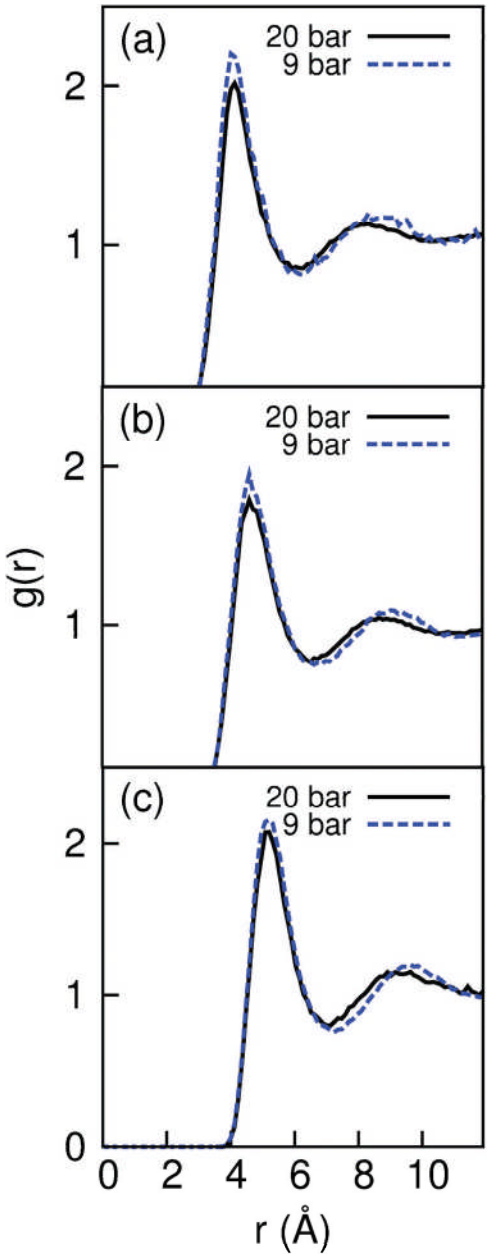

Fig. 3 The effect of pressure on radial distribution functions of the CO_2–CO_2 (a), CO_2–R134a (b), and R134a–R134a (c) interactions in the liquid mixture at 272 K.

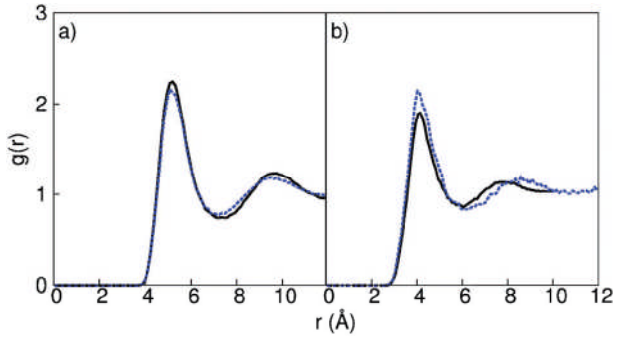

Fig. 4 Radial distribution functions of (a) R134a in the pure liquid (solid line) and in the R134a + CO_2 mixture (dashed line) and (b) CO_2 in the pure liquid (solid line) and in the R134a + CO_2 mixture (dashed line) at 272 K and 11 bar.

solvation shell decreases, which implies that the structures of neighbouring molecules are disrupted at high pressures. The CO_2–CO_2 and R134a–R134a interactions are ordered to a similar extent and are more ordered than CO_2–R134a, as indicated by the height of the peaks of the first solvation shell. Fig. 4 compares the RDFs of R134a and CO_2 molecules in the pure liquids and in the mixture at 272 K and 11.55 bar. The presence of CO_2 slightly perturbs the structure of R134a liquid, but the presence of R134a has a larger influence on the structure of CO_2 (Fig. 4b).

In the pure liquids, the average coordination numbers in the first solvation shell for both are 12.[46,50] In the mixture, the average coordination number of the first solvation shell of the R134a–R134a interaction is eight and that of the R134a–CO_2 interaction is three, making a total of 11 nearest neighbours for R134a. The average coordination number of the first solvation shell of CO_2–CO_2 is one and that of CO_2–R134a is seven, making a total number of eight nearest neighbours for CO_2. The distributions of the coordination number of R134a and CO_2 are shown in Fig. 5. The coordination number of the first solvation shell of R134a is distributed about a straight line whose sum of x and y values gives the mean value of the coordination number of R134a (Fig. 5a). However, this relationship is not necessarily true for an arbitrary system. In our case, the equation of the line is $x + y = 11.5$. Similarly, the coordination number of the first solvation shell of CO_2 is

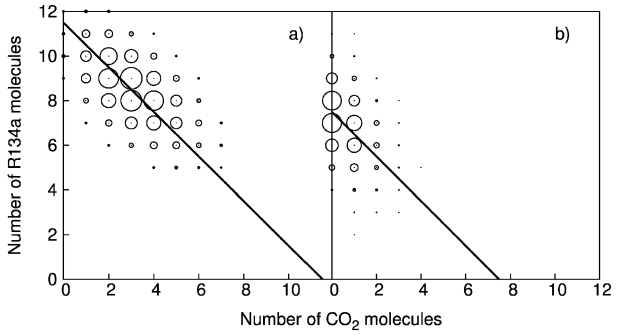

Fig. 5 Distributions of the coordination number: (a) central molecule is R134a and (b) central molecule is CO_2 at 272 K and 11.55 bar. The bigger the circle is, the higher the probability of occurrence. Lines are $x + y = 11.5$ (a) and $x + y = 7.5$ (b).

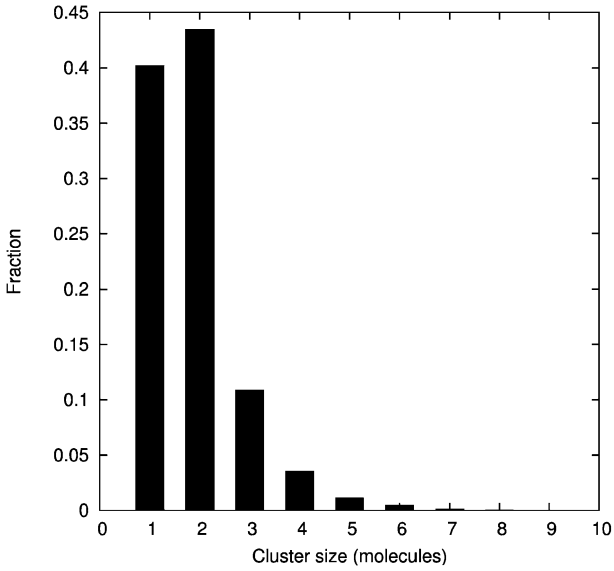

Fig. 6 Distributions of the cluster size of the CO_2 solute in the R134a solvent at 272 K and 11.55 bar. This distribution is probability related to clusters not molecules. The fraction of clusters of a given size is shown with respect to the total number of clusters.

distributed about the line $x + y = 7.5$. The mixture at 272 K and 11.55 bar has about 30% CO_2 and 70% R134a by mole. Therefore, CO_2 can be thought as a solute and R134a can be thought as a solvent. This prompts the question: what is the dominant solute CO_2 cluster size? To answer this, we analyse the probability distributions of the size of the CO_2 clusters in the mixture (Fig. 6). We define two CO_2 molecules to be in the same cluster, if they are within a distance (C–C distance) corresponding to the first solvation shell. Fig. 6 shows that clusters of one and two CO_2 molecules are the most dominant; clusters of two are most populated. The clusters of three are about four times less likely than the clusters of two, and clusters of four are observed about three times less often than clusters of three. Clusters of five, six, and seven molecules are rarely found. A percolating cluster would occur if the periodic images of a central molecule were also in the same cluster with it, but such an instance was not found.

We use orientational distribution functions (ODFs) to characterize the environments around each type of molecule in the liquids. We first look at the arrangement of CO_2 molecules, and then examine the alignment of CO_2 and R134a, and finally we investigate the arrangement of R134a molecules. Fig. 7 shows the distribution of the angles between a CO bond of CO_2 and the C–C vector from CO_2 to CO_2 (Fig. 7a) for the mixture and the distribution of the angles of the CO bonds of different CO_2 molecules (Fig. 7b). Fig. 7a can be interpreted as a spatial distribution of the neighbours around the central CO_2 molecule. We see a large peak at a distance of 4.2 Å (position of the first solvation shell of CO_2) and an angle of 90°, which means the CO bonds make a right angle with the plane that contains a C–C vector at a C–C distance of 4.2 Å. We can also observe two other peaks at angles of 0° and 180° (at about the same distance). Thus, we can conclude that the neighbouring CO_2 also prefer to stay at the top and at the bottom of the central CO_2 molecule.

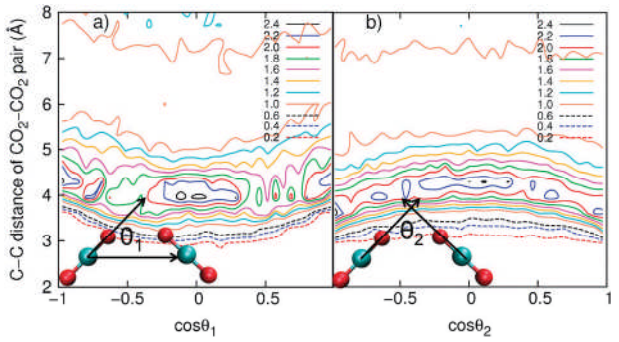

Fig. 7 Distribution of the angles between (a) CO vector and C–C vector from CO_2 to CO_2 (θ_1) and (b) CO vectors (θ_2) in R134a + CO_2 liquid mixture at 272 K and 11 bar. The vertical axis is the distance between CO_2 molecules, measured from carbon atom to carbon atom.

Fig. 7b gives details of the preferred orientation of these neighbours. A large peak is observed at about 4.2 Å and about 90°, which suggests that the CO bonds of neighbouring CO_2 molecules are perpendicular to each other at this distance. This means that at a separation of about 4.2 Å, the preferred orientation of CO_2 molecules in the mixture is a T-shaped geometry. However, it is not as dominant as in pure liquid CO_2.[46] The peak corresponding to the T-shaped geometry (Fig. 7b) is quite broad, which means other angles apart from 90° are also populated. Also, a small proportion of the slipped-parallel geometry is preferred at short distance, as indicated by two small peaks at about 3.5 Å and 0° and 180°. This is also found for CO_2 in the CO_2 + CH_2F_2 liquid mixture.[46] The slipped-parallel structure is not found in either pure liquid CO_2 or the CO_2 + CH_4 mixture.[46] Therefore, R134a has some influence on the structure of CO_2 as seen in the RDFs (Fig. 4).

For convenience, we identify the centre of the R134a molecule (CoCC) as the midpoint of the CC bond rather than the molecular centre of mass. To have a picture of the relative position (spatial distribution) of CO_2 molecules around R134a molecules, we calculate the distribution of the angles between the CC vector of R134a and the CoCC–C distance from R134a to CO_2 (Fig. 8a). There is a peak at about 4.3 Å and 90°. At about 4.8 Å, there also appear two other lower peaks, at about 0° and about 180°. Thus, these vectors have a preference for 90°, and also a preference for both parallel and antiparallel alignments. In other words, in the first solvation shell of R134a, the neighbouring CO_2 molecules preferentially locate on a circle of radius 4.3 Å centred at the midpoint of the CC bond of R134a molecules, in the plane perpendicular to the CC bond of R134a molecules. They also populate the space above and below R134a molecules. Fig. 8b shows the distribution of the angles between the CC bond of R134a and the CO bond of CO_2. A peak appears at an R134a–CO_2 distance of about 4.5 Å and an angle of 90° indicating that these vectors have a preference for a T-shaped alignment. Fig. 8c shows the distribution of the angles between the dipole of R134a and the CO bond of CO_2. There is no clear pattern of orientation for these vectors, as a broad peak ranging from 0° to 180° can be found at about 4.5 Å.

To investigate the orientational distribution of the neighbouring R134a molecules in the first solvation shell of R134a, we use a technique employed in our previous work.[50] These analyses, discussed in the ESI†, show that the orientational distribution of neighbouring R134a molecules around a central R134a molecule is the same as that in the pure R134a liquid,[50] which agrees with the RDFs. The ODFs confirm that the presence of CO_2 under these conditions does not alter the structure of R134a.

IV. Conclusion

For the first time, a new empirical force field for R134a is mixed with the well-known EPM force field for CO_2 to predict the VLE data for the binary system of R134a + CO_2. The system is simulated using the NPT-GEMC technique. In addition, the coupled–decoupled CBMC technique is employed to sample the conformation of R134a and enhance the efficiency of the simulations. The combination of these two force fields with a simple mixing rule gives good agreement with experimental data for the VLE properties of the R134a + CO_2 binary mixture.

The pair interaction energy distributions show that R134a–R134a, R134a–CO_2, and CO_2–CO_2 interactions all have a shoulder on the attractive side of the main peak. These attractive interactions occur at short contact distance and correspond to the first solvation shells. All pairwise interactions in the R134a + CO_2 mixture are sensitive to pressure at low temperature. The RDFs and ODFs reveal that pairs of CO_2 molecules not only adopt a T-shaped geometry, but also adopt a slipped-parallel structure at short C–C separations (about 3.5 Å) in the liquid R134a + CO_2 mixture at 272 K + 11.55 bar. This is observed for CO_2 in the liquid mixture CO_2 + CH_2F_2,

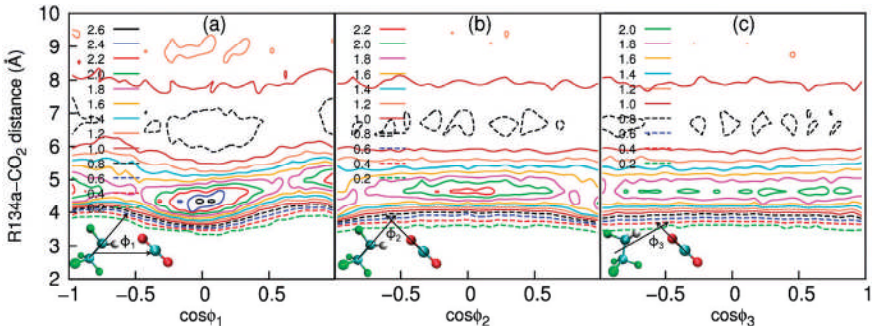

Fig. 8 Distribution of the angles between (a) C2C3 vector and R134a–CO_2 (CoCC–C) vector (ϕ_1), (b) C2C3 vector and CO vectors (ϕ_2), and (c) dipole vector of R134a and CO vector in R134a + CO_2 liquid mixture at 272 K and 11 bar. The vertical axis is the distance between CO_2 and R134a molecules, measured carbon atom of CO_2 to the centre of the CC bond of R134a.

but not in pure CO_2 nor in the mixture CO_2 + CH_4.[46] The presence of CO_2 in the R134a + CO_2 mixture does not influence the structure of R134a, which is also the case for liquid mixture CO_2 + CH_2F_2. The dipole moments of R134a of the nearest neighbours in the first solvation shell have a preference for the parallel alignment (ESI†). This is also a characteristic of liquid CH_2F_2. The average coordination number of the first solvation shell of CO_2 is eight and that of the first solvation shell of R134a is 11. CO_2 prefer to form clusters of one or two molecules in the mixture.

Force fields are indispensible for simulations. In fact, accurate thermophysical properties of a particular system can only be achieved if there is a force field that accurately describes the intermolecular interactions of that system. A combination of the empirical force fields and mixing rules is a convenient approximation to calculate thermophysical properties of systems of interest, but the transferability of this approximation is limited, *i.e.*, there is no guarantee that this method works for every unlike interaction in different mixtures. Therefore, we should calculate the force field parameters for every single interaction in the system. This can be achieved from first-principles quantum mechanical calculations. Although there are not many such force fields available for the calculation of thermophysical properties, we expect to see more in the future, as computing speed increases rapidly. Some efforts have been made along these lines.[56,57] Nevertheless, the empirical force fields employed in our work give satisfactory agreement with experiment for VLE properties, and also gives us the opportunity to analyze for the first time the microscopic structure of mixture R134a + CO_2—an important industrial mixture.

Acknowledgements

We thank the University of Nottingham High Performance Computing facility for providing computer resources and the Engineering and Physical Sciences Research Council (EPSRC) for funding (Grant No. EP/E06082X). We thank Dr Mark Oakley, Prof. Martyn Poliakoff, and Dr Jie Ke for useful discussions. Hainam Do is grateful to the EPSRC for a PhD Plus Fellowship.

References

1 C. Duran-Valencia, G. Pointurier, A. Valtz, P. Guilbot and D. Richon, *J. Chem. Eng. Data*, 2002, **47**, 59–61.
2 D. Y. Peng and D. B. Robinson, *Ind. Eng. Chem. Fundam.*, 1976, **15**, 59.
3 J. I. Siepmann, S. Karaborni and B. Smit, *Nature*, 1993, **365**, 330.
4 A. Z. Panagiotopoulos, *Mol. Phys.*, 1987, **61**, 813.
5 A. Z. Panagiotopoulos, N. Quirke, M. Stapleton and D. J. Tildesley, *Mol. Phys.*, 1988, **63**, 527.
6 D. Frenkel and B. Smit, *Understanding Molecular Simulation: from Algorithms to Applications*, Academic Press, San Diego, 2002.
7 D. A. Kofke, *Mol. Phys.*, 1993, **78**, 1331–1336.
8 D. A. Escobedo and J. J. de Pablo, *J. Chem. Phys.*, 1996, **105**, 4391.
9 J. J. Potoff and A. Z. Panagiotopoulos, *J. Chem. Phys.*, 1998, **109**, 10914.
10 F. G. Wang and D. P. Landau, *Phys. Rev. Lett.*, 2001, **86**, 2050.
11 F. G. Wang and D. P. Landau, *Phys. Rev. E: Stat. Phys., Plasmas, Fluids, Relat. Interdiscip. Top.*, 2001, **64**, 56101.
12 C. R. A. Abreu and F. A. Escobedo, *J. Chem. Phys.*, 2006, **124**, 54116.
13 J. R. Errington, *J. Chem. Phys.*, 2003, **118**, 9915.
14 G. Gazenmuller and P. J. Camp, *J. Chem. Phys.*, 2007, **127**, 154504.
15 Q. Yan, R. Faller and J. J. de Pablo, *J. Chem. Phys.*, 2002, **116**, 8745.
16 M. S. Shell, P. G. Debenedetti and A. Z. Panagiotopoulos, *Phys. Rev. E: Stat. Phys., Plasmas, Fluids, Relat. Interdiscip. Top.*, 2002, **66**, 56703.
17 M. S. Shell, P. G. Debenedetti and A. Z. Panagiotopoulos, *J. Chem. Phys.*, 2003, **119**, 9406.
18 F. A. Escobedo and C. R. A. Abreu, *J. Chem. Phys.*, 2006, **124**, 104110.
19 N. A. Wilding, *Am. J. Phys.*, 2001, **69**, 1147.
20 J. I. Siepmann and D. Frenkel, *Mol. Phys.*, 1992, **68**, 931.
21 D. Frenkel, G. C. A. M. Mooji and B. Smit, *J. Phys.: Condens. Matter*, 1992, **4**, 3053.
22 J. J. de Pablo, M. Laso and U. W. Suter, *J. Chem. Phys.*, 1992, **96**, 2395.
23 T. Kristof and J. Liszi, *J. Phys. Chem. B*, 1997, **101**, 5480.
24 J. Delhommelle, P. Millie and A. H. Fuchs, *Mol. Phys.*, 2000, **98**, 1895.
25 G. Kamath, N. Lubna and J. J. Potoff, *J. Chem. Phys.*, 2005, **123**, 124505.
26 S. T. Cui, P. T. Cummings and H. D. Cochran, *Fluid Phase Equilib.*, 1997, **141**, 45.
27 N. D. Zhuravlev and J. I. Siepmann, *Fluid Phase Equilib.*, 1997, **134**, 55.
28 B. Neubauer, J. Delhommelle, A. Boutin, B. Tavitian and A. H. Fuchs, *Fluid Phase Equilib.*, 1999, **155**, 167.
29 N. D. Zhuravlev, M. G. Martin and J. I. Siepmann, *Fluid Phase Equilib.*, 2002, **202**, 307.
30 W. L. Jorgensen, *J. Phys. Chem.*, 1986, **90**, 1276.
31 S. K. Nath, F. A. Escobedo and J. J. de Pablo, *J.Chem. Phys.*, 1998, **108**, 9905.
32 M. G. Martin and J. I. Siepmann, *J. Phys. Chem. B*, 1998, **102**, 2569–2577.
33 N. Rai and J. I. Siepmann, *J. Phys. Chem. B*, 2007, **111**, 10790.
34 J. M. Stubbs, J. J. Potoff and J. I. Siepmann, *J. Phys. Chem. B*, 2004, **108**, 17596.
35 B. Chen, J. J. Potoff and J. I. Siepmann, *J. Phys. Chem. B*, 2001, **105**, 3093.
36 M. Lisal and V. Vacek, *Fluid Phase Equilib.*, 1997, **127**, 83–101.
37 M. Lisal, R. Budinskey, V. Vacek and K. Aim, *Int. J. Thermophys.*, 1999, **20**, 163–174.
38 M. Fermeglia, M. Ferrone and S. Pricl, *Fluid Phase Equilib.*, 2003, **210**, 105–116.
39 R. Budinskey, V. Vacek and M. Lisal, *Fluid Phase Equilib.*, 2004, **222**, 213–220.
40 J. Stoll, J. Vrabec and H. Hasse, *J. Chem. Phys.*, 2003, **119**, 11396.
41 J. Vrabec, Y. Huang and H. Hasse, *Fluid Phase Equilib.*, 2009, **279**, 120–135.
42 J. G. Harris and K. H. Yung, *J. Phys. Chem.*, 1995, **99**, 12021–12024.
43 R. P. S. Peguin, L. Wu and S. R. P. da Rocha, *Langmuir*, 2007, **23**, 8291–8294.
44 R. P. S. Peguin, G. Kamath, J. J. Potoff and S. R. P. da Rocha, *J. Phys. Chem. B*, 2009, **113**, 178–187.
45 J. Vorholz, V. I. Harismeadis, B. Rumpf, A. Z. Panagiotopoulos and G. Maurer, *Fluid Phase Equilib.*, 2000, **170**, 203.
46 H. Do, R. J. Wheatley and J. D. Hirst, *J. Phys. Chem. B*, 2010, **114**, 3879–3886.
47 Y. Zhang, J. Yang and Y. Yu, *J. Phys. Chem. B*, 2005, **109**, 13375–13382.
48 A. Idrissi, P. Damay and M. Kiselev, *Chem. Phys.*, 2007, **332**, 139.
49 A. Idrissi, I. Vyalov, P. Damay, A. Frolov, R. Oparin and M. Kiselev, *J. Phys. Chem. B*, 2009, **113**, 15820–15830.
50 H. Do, R. J. Wheatley and J. D. Hirst, *Phys. Chem. Chem. Phys.*, 2010, **12**, 13266–13272.
51 P. Jedlovszky, *J. Chem. Phys.*, 1997, **107**, 562.
52 P. Jedlovszky and M. Mezei, *J. Chem. Phys.*, 1999, **110**, 2991–3002.
53 I. Skarmoutsos and J. Samios, *J. Mol. Liq.*, 2005, **125**, 181–186.
54 M. G. Martin and J. I. Siepmann, *J. Phys. Chem. B*, 1999, **103**, 4508–4517.
55 M. P. Allen and D. J. Tildesley, *Computer Simulation of Liquids*, Clarendon Press, Oxford, 1987.
56 M. T. Oakley and R. J. Wheatley, *J. Chem. Phys.*, 2009, **130**, 034110.
57 M. T. Oakley, H. Do and R. J. Wheatley, *Fluid Phase Equilib.*, 2009, **290**, 48–54.